Available online at www.sciencedirect.com

ScienceDirect

Procedia Manufacturing 48 (2020) 663–670

Procedia MANUFACTURING

www.elsevier.com/locate/procedia

48th SME North American Manufacturing Research Conference, NAMRC 48 (Cancelled due to COVID-19)

A Study of Different Deposition Strategies in Direct Energy Deposition (DED) Processes

Kandice S. B. Ribeiro[a], Fábio E. Mariani[b], Reginaldo T. Coelho[b]*

[a]*Department of Mechanical Engineering, São Carlos School of Engineering, University of São Paulo, Av. Trabalhador São-Carlense, 400 – Parque Arnold Schimidt, São Carlos, 13566-590, Brazil*

[b]*Department of Production Engineering, São Carlos School of Engineering, University of São Paulo, Av. Trabalhador São-Carlense, 400 – Parque Arnold Schimidt, São Carlos, 13566-590, Brazil*

* Corresponding author. Tel.: +55-16-3373-9267; fax: +55-16-3373-9214. *E-mail address:* rtcoelho@sc.usp.br

Abstract

The stepover of adjacent deposition lines (or beads), when stacking layers to build a 3D-solid shape, is found to be of great importance to minimize voidage and so, improving density of parts produced by the Directed Energy Deposition (DED) process. During such process, in which the stacking of layers occurs, the complex thermal activity of metal deposition affects the part geometry, microstructure, physical and mechanical properties. The correlation between deposition path, bead stepover, and the direct effect on the part density, microstructure and geometry distortions are yet to be found in the literature. Therefore, the aim of this study is to evaluate the effect of deposition paths and bead stepover on the final part geometry form, microhardness and density. In order to do so, four deposition paths (linear, zigzag, chessboard and contour) and beads stepover of 0.44 mm and 0.55 mm were performed on the production of Stainless Steel 316L cubes by a 5-axis laser based DED BeAM Machine Magic800 with laser spot size of 0.80 mm. The paths shown considerable influence on the variation of both final part geometry and density. Contour (spiral-like) was the path, which produced workpieces with finer form and finishing, with density and microhardness closer to the conventional AISI 316L material. The bead stepover was also found to influence the surface finishing, as larger critical valleys between adjacent beads were noticed when using the higher stepover value.

Keywords: Directed Energy Deposition; Toolpath strategies; Density analysis; Microstructure.

1. Introduction

Directed Energy Deposition (DED) process is an Additive Manufacturing (AM) process, in which a focused thermal energy source fuses material, in general metallic powder, or wire, by melting them during layer-by-layer deposition [1]. Such technology makes new metallic components, starting from a substrate, as well as, it repairs and rebuilds damaged and worn parts. This process is also well suited to make functionally graded material (FGM) used in several fields, such as, aerospace, military and medical. [2]. It can deposit many materials, including titanium-, nickel-, and iron-based, besides stainless steel with a relatively high deposition rate, compared to other AM processes. Moreover, it tends to produce a minor heat affected zone (HAZ), compared with welding repairing applications. [3]

The laser based DED is a result of several parameters interaction in a very complex phenomenon. Parameters involving the laser, the motion system and the material feeder are relatively stable in a commercial equipment. The manufacturer normally supplies those in a recipe, after extensive tests and improvements [4]. Other parameters related to the process, specifically the deposition pattern, are also important. Its selection is a key decision to obtain a good quality deposition.

The basis for deposition strategies (paths) follows CAM (Computer Aided Manufacturing) software recommendations, normally applied in milling operations. AM processes, such as DED, start with those paths, but new requirements arise when

10.1016/j.promfg.2020.05.158

layers must be stacked. The overlapping of adjacent deposition lines (or beads) at the same layer, although its similarity to lateral cuts in milling, become important to minimize voidage and so improving density in DED produced parts. Furthermore, the complex thermal activity of newly deposited layers and its influence in previous deposited material has great effect on the part microstructure. Overall, the selected deposition path has a strong influence on the density and microstructure resulted from DED process.

Porosity, for example, is a defect often found in AM products, because of temperature changes, gravity and capillary forces. Irregularly shaped pores are due to shrinkage, lack of binding/fusion/melting, or material feed shortage, often occurring at the border of molten beads. Spherical pores are due to trapped gases, Marangoni turbulences in the melt region, material evaporation, etc., often occurring within the molten beads [5, 6].

Therefore, the present work brings a comprehensive study covering new strategies (paths) to build a 3D-solid metal workpiece using DED process. It evaluated the influence of several deposition paths and beads stepover on the dimensions and forms of parts. Additionally, it assessed microhardness and density of the material obtained with each trial. The most recent model of a 5-axis laser-based DED equipment, using a coaxial nozzle, is used for such study. Good quality material and excellent dimension and geometry were achieved with the combination of parameters carefully chosen.

2. Deposition patterns and stacking strategies

Most of the deposition strategies (paths) nowadays used by AM processes follows those used in CAM software, e.g. for milling operations. The principle behind the used paths remains the same, since removing layers of material is alike adding them. However, new aspects arise, such as solid slicing, overlapping between adjacent beads, laser spot size, bead cross section, etc, which directly affects the thermal activity during the build of the 3D piece. All those parameters have to be optimized aiming at microstructure improvements, such as, minimizing porosity, therefore increasing density; achieving better mechanical properties; minimizing distortion and thermal stresses. Thus, selecting proper paths in AM processes still remains of primary importance. It is not only for minimizing fabrication time, as in milling, but also to achieve good material quality.

Parimi et al. [7] experimentally assessed IN718 microstructures in DED process. Two patterns were used: a unidirectional and a bidirectional deposition path. Laser power also changed from 390 to 910 W. Porosity levels varied from 0.2% to 0.8% when increasing laser power, affecting the resulting density [7]. Michel et al. [8] obtained a uniform filling of complex and thick wall geometries using a Modular Path Planning (MPP) working with arc-welding DED [8]. Li et. al. [9] studied and proposed a strategy to overlap successive layers when building a 3D object by arc-wire DED. Such strategy could produce microstructures almost free of porosity [9]. Gong et. al. [10] used a hybrid machine (DED and milling) to produce 3D-solid pieces. Those authors used raster strategy on each layer and 90° rotation for each successive layer. Density and porosity varied and were found to be related to laser energy per deposited volume. They found that the higher the energy, the denser resulted the material.

Therefore, a right balance between laser power and feed speed must be found to reach a homogenous temperature distribution. When the powder material has high thermal conductivity, a spiral path (contour like) resulted in more uniform temperature distribution [10]. The chessboard pattern, often used in powder bed fusion (PBF) process, can also provide a more uniform temperature distribution [11]. In most of such cases, the best deposition paths were those leading to low temperature gradients. The raster path, for example, is the most commonly used mainly due to its ease implementation. It is not dependent on the shape of the cross section; thus, it attends a variety of shapes, thin or thick ones.

Yu et. al. [12] tested three common paths, raster, offset-in, offset-out, and compared them to a fourth one, a fractal pattern. The fractal and offset-out paths produced the best results because they generate a more uniform temperature distribution. The work also found best results with 50% overlapping between parallel-deposited beads [12]. Dai and Shaw [13] used Finite Element Methods (FEM) simulation to assess different strategies and found the best results when changing the directions of the heat source as layers are stacked [13]. Therefore, raster path can be used as a DED strategy within a layer, but may not be the best, depending on the thermal distribution, which is related to bead length, feed speed, bead overlapping and laser on-off at the end of each bead [12, 13].

Ravi et. al. [14] investigated microstructure and mechanical properties of SC420 stainless steel deposited and HIPed (hot-isostatic pressed). Raster, or zigzag, in X and Y direction was used and variation in mechanical properties was related with thermal history, which can be reduced by modifying deposition path and laser power, for example [14].

When producing thin or thick cross sections, planning deposition path to fill them up is important to obtain desired mechanical properties and material density. Djuric and Urbanic [15] studied deposition trajectories for a future CAM software. The authors suggest considering, when planning a path, the minimization of discontinuities, or stop and starts, as well as heating/cooling. Developing algorithms with minimum speed variation based on Bézier curves, minimizing feed speed variations in DED process is another important parameter to keep a uniform bead and layer. Although such principles serve well for painting, glue and fused deposition modelling (FDM) process, it suits DED applications too, aiming at uniform material density, wherever required [15, 16].

Some other strategies to fill up a layer were proposed using wire-fed welding, such as, adaptive path planning using medial axis transformation (MAT) algorithm and water-pouring rule. Authors have found that continuous closed loop paths with varying overlapping could produce high accuracy void-free deposition, therefore improving density. When compared to traditional raster methods, this strategy reduced the number of stopping points from 18 to 1 and made the deposition path continuous for a workpiece, which might result in higher density. More complexes strategies are also being proposed for applications in complex geometries [8, 17, 18].

In most of the applications in AM, the slicing of the 3D solid objects occurs in a planar way. However, DED process sometimes needs to add a feature to an existing shape or build overhang structures and curved parts. To reduce the need for support structures and decrease the number of planar layers, nonplanar slicing may be more productive, specially to homogenize temperature on the whole piece [19]. Even for FGM deposition patterns filling thick or thin sections have to be considered separately [20].

When assessing deposition quality in DED, density measurement methods play an important role. Spierings et al. [21] investigated different methods specifically applied to metallic parts obtained by AM processes. Authors have found that using water or acetone and considering the buoyancy of the part in air, the results for volume measurement are very reliable, for Archimedes method. However, some doubts arise when measuring low-density materials, e.g. plastics [21].

Much research work is still needed to find the adequate deposition path on a layer and new strategies for layer stacking in order to obtain a high-quality material by DED process. This is even more challenging for a part with complex geometry. In this perspective, density is one of the main quality features, being geometric accuracy and minimum energy consumption also important.

3. Methodology

In order to evaluate the influence of pathway and overleaping in final part geometry, density and microstructure of DED deposited parts, workpieces in the shape of cubes with 16 mm side were deposited on ∅25 mm stock. The deposition experiments were performed at BeAM Inc., in Cincinnati, Ohio, on the DED BeAM machine Magic 800, SN004, with laser spot of 0.8 mm.

The powder used in this study is a commercial Stainless Steel (SS) AISI 316L produced by Powder Alloy Corporation. This powder is spherical in morphology with particle size ranging from 44 to 88 μm, as shown in Figure 1.

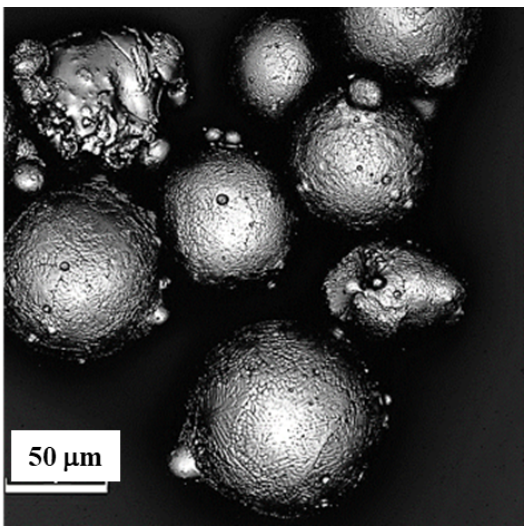

Fig. 1. Stainless Steel AISI 316L powder.

Based on previous tests, the travel speed was set at 2000 mm/min, with powder feed rate of 5 g/min and 600 W of laser power – all remaining constant throughout the process. With such conditions, the overall bead width and height resulted in 0.8 mm and 0.3 mm, respectively. Therefore, a constant increment of 0.3 mm in axis Z was applied between each layer. When higher workpiece is built, Z increments probably has to be adjusted, since layer thickness tends to decrease as they are stacked. It has also been verified that small variations (up to 0.5 mm) around the laser focal point does not significantly change the laser spot size and bead geometry, even when considering the variation of stepover within our narrow range. The optimum focal distance for both powder and laser was 3.5 mm.

Deposition was carried out in ambient atmosphere with local argon shielding delivered by a coaxial nozzle at the rate of 6 L/min. Argon was also used as nozzle and carrier gas, set at the rate of 3 L/min and 5 L/min, respectively.

Four different deposition strategies were considered as pathways, labeled A, B, C and D with respect to linear, zigzag, chessboard and contour raster strategies, respectively, as shown in Figure 2.

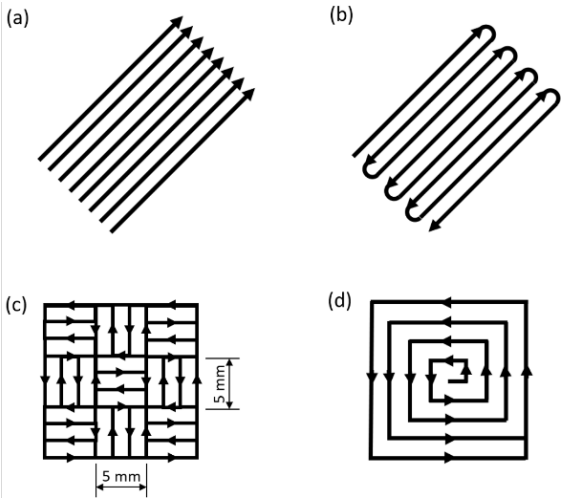

Fig. 2. Deposition strategy: (a) linear, (b) zigzag, (c) chessboard and (d) contour.

These deposition paths were performed with bead stepovers of 0.44 mm and 0.55 mm through each single layer, as shown in Figure 3. Such values were defined based on previous tests, which revealed that below 0.44 mm there was no significant gain in density and above 0.55 mm the above layer profile could induce porous between layers. It can be noted that the overleaping area reduces as the stepover increases, and that may lead to deeper critical valleys in larger than 0.55 mm stepover.

The trajectory rotates layer by layer in 67º for strategies A and B, and 90º for strategy C, whilst D did not use any raster rotation. Two pieces were made of each strategy and each stepover, in a total of 16 pieces. Concerning the thermal activity during deposition with different strategies and its influence on the final part, flatness, surface roughness, microhardness and geometrical analysis were carried out on each workpiece.

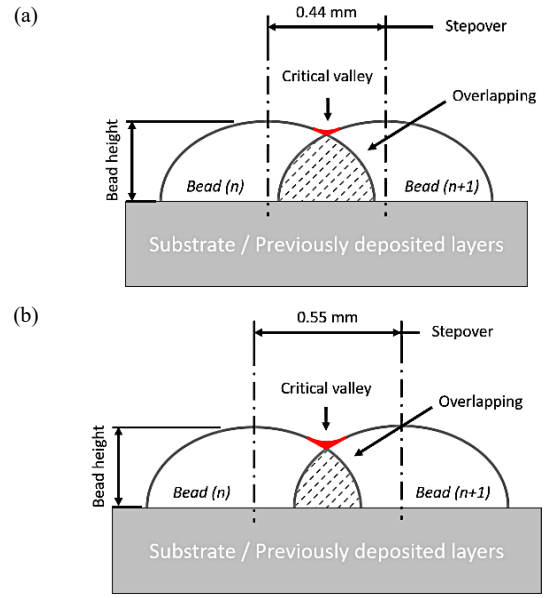

Fig. 3. Schematic showing the two different stepovers used and its influence on the bead overlapping.

For this purpose, a Buehler microhardness tester (model 1600-6300) was used to measure microhardness Vickers (HV) with the load of 1 kgf at five different regions in the cross-section of the workpieces – same considered to microstructural analysis. The regions defined represented the center, top, right, left and bottom of the cross-section, being the bottom the first layers above the workpiece-substrate interface. Three measures at each region were taken, and the overall microhardness data is presented and discussed ahead.

Regarding the flatness and surface finishing, a laser 3D scanning digital microscope Olympus OLS4100 was used. The analysis area for flatness was defined as a quarter of the cubic form, whereas for roughness a central area was evaluated, so there would be not much influence from the flatness. The roughness height parameter evaluated in this work were the average media, as absolute value, Sa. The cut-off selected was 8 mm as defined in the roughness standard DIN EN ISO 4288 – ASME B46.1. The overall cube dimensions were measured by a 0.02 mm resolution caliper, considering the maximum dimensions of height.

The density analysis used machined workpieces of Ø10x10 mm. The volume was calculated by measuring the workpiece dimensions with a micrometer (0.001 mm resolution). Therefore, the density values were determined by relating the mass weighted in a precision scale Marte AD200 and the volume from each deposited condition. This method has shown more accuracy to measure volume. Calculating volume by Archimedes principle is yet to be performed in future work.

Later, the workpieces were sectioned in half to analyze the square cross-section microstructure achieved throughout the layers of the different strategies. Metallographic samples were initially mechanically polished using SiC paper from 120 to 2000 grit, followed by a slurry of 0.25 µm diamond particles. For microstructural analysis, the samples were etched with Aqua Regia (nitric acid and hydrochloric acid in a molar ratio of 1:3) reagent for 120 s. The microstructural features from the samples were then observed in a laser 3D scanning digital microscope Olympus OLS4100.

4. Results and discussion

Table 1 shows the results on the workpieces final dimensions and the flatness data.

Major differences amongst the workpieces were found in their height, measured at the highest point achieved by deposition. Pieces using stepover of 0.44 mm melts a larger strip form the adjacent bead and, therefore, results in slightly higher individual layer. When that small difference is added to the set of 50 layers at each workpiece, the final piece results taller.

Table 1. Average deposited dimensions.

Raster strategy	Stepover (*mm*)	Length (*mm*)	Width (*mm*)	Height (*mm*)	Flatness (*µm*)
Linear	0.44	16.00	16.00	15.65	1872
	0.55	16.00	16.00	14.00	4488
Zigzag	0.44	16.10	16.10	15.50	1912
	0.55	16.00	16.00	14.85	2333
Chessboard	0.44	16.10	16.10	16.00	1909
	0.55	16.05	16.05	15.10	4803
Contour	0.44	16.50	16.50	16.10	1351
	0.55	16.00	16.00	15.80	1457

The overall external shape of obtained cubes is shown in Figure 4 with combination of deposition strategies A, B, C and D with the stepover of 0.44 and 0.55 mm.

From Figure 4, it can be noted that, in general, depositions using 0.44 mm stepover resulted in better cubic shapes. The pieces produced with 0.55 mm stepover presented higher values of flatness, as one can see in Table 1. Also, the best deposition strategy to produce flatter cubic shapes has shown to be contour within the ones evaluated in this study; whilst chessboard with 0.55 mm stepover was the worst. When using wider stepover (0.55 mm) the melting pool is predominantly formed on the previous layer and a narrower strip of the adjacent bead is melted. Therefore, less powder might be captured by the pool, since it results wider. Such effect is probably aggravated at the borders and edges. When using narrower stepover (0.44 mm) the melting pool forms using a wider strip from the adjacent bead and has a wall left by it. Such melting pool might result more concentrated and deeper with more capacity to absorb powder and produce a flatter surface.

Because the kinematic system in all CNC machines makes them slowdown in every corner and direction change, laser stays slightly longer time at those points. In linear, zigzag and chessboard strategies, slowdown points coincide with edges or corners repeatedly at the same layer. Those points received more heat and were kept at higher temperatures longer than others at the same layer. Such points probably experienced melting for more than once, which led to lower layer thickness and, consequently shorter than other points. Furthermore, at corners only approximately ¼ of melt pool area is actually on

the deposition area, reducing solidified volume at those particular points.

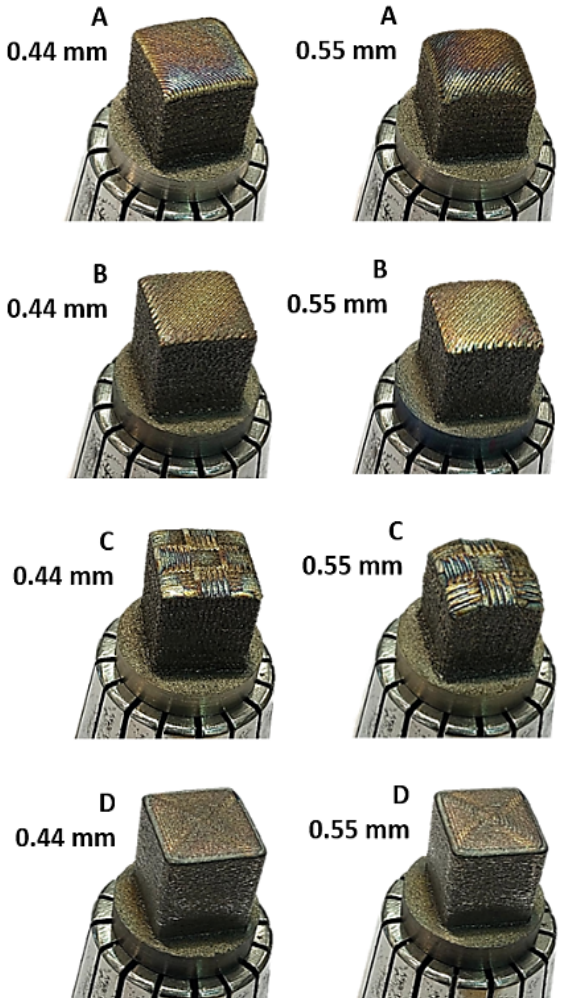

Fig. 4. Deposited workpieces in each of the deposition strategies and stepover in perspective view.

With the contour (helical-like) strategy, heat is initially put at the center of the layer, which uniformly distributes it thought the preceding layer and to the argon flow. The melt pool is also disturbed by the powder and gas flow at the layers on the edge, but that happens just once at every layer. Therefore, the upper face of the cubes built using contour strategy resulted much flatter than all other and, especially when using stepover of 0.44 mm.

Regarding the path strategies and the final geometry difference between the sets of 0.44 mm and 0.55 mm stepover, contour toolpath (D) had the better performance, followed by zigzag (B), chessboard (C) and linear (A). The heat distribution for these patterns can also support this result, as the more uniformly distributed the heat transfer over the workpiece trajectory, the less distortions in geometry are found. Comparing different strategies heights are relatively equals considering that DED is to produce parts to be machined.

Typical micrography from the top surface (last deposited layer) were taken at the central region for all workpieces and are presented in Figure 5. The presence of adhered powders on the workpiece surface can be seen on all pieces. The colors can also be related to the thermal reheating cycles that pieces experienced during fabrication.

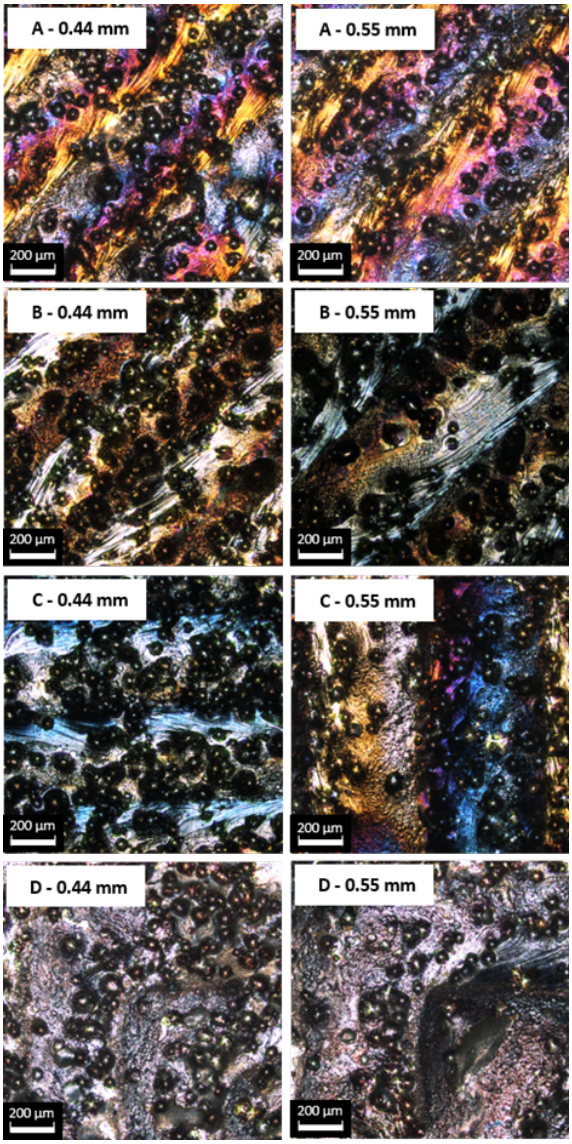

Fig. 5. Typical micrography of top layer in central region.

Furthermore, it can be noticed the aspect on finishing, mainly on the contour strategy with 0.55 mm stepover, where it can be seen a deeper region between both pathways exactly on the corner. This is potentially due to the kinematic of the machine while performing corners, where it must stop one axis and start another at 90°. Therefore, this typical surface aspect of DED produced parts reinforces the need for post processing by machining, high quality polishing, grinding, etc. before coming to the final application of a typical mechanical part. The average roughness values are shown in Figure 6.

Overall data on area roughness (Sa) have shown that the major roughness levels were obtained with the stepover of 0.55 mm. Such result has influence from the critical valley left between adjacent layers, once larger stepover leads to bigger critical valley regions.

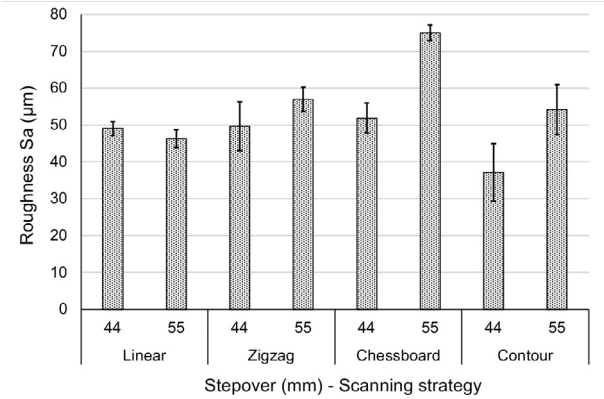

Fig. 6. Surface roughness of the produced workpieces.

Roughness levels have no significant difference between linear and zigzag strategies with stepover of 0.44 mm, as the main difference between both strategies stays at the edge of the workpiece. Concerning the combination of stepover and scanning strategy, using chessboard with 0.55 mm stepover produced the highest Sa value whilst contour with 0.44 mm promoted the best finishing (Sa 37 µm) to the produced part.

In terms of quality of the deposited AISI 316L material, the density data achieved for each tested condition is presented in Tab. 2. It can be highlighted that the workpieces produced with 0.55 mm have shown to be denser than the ones deposited with 0.44 mm stepover, apart from the linear strategy, in which results have shown otherwise. Stepover of 0.55 mm results in thin layers, which can be more susceptible to be melted when depositing an upper layer. That can lead to a material denser and with less voids and pores. Also, the contour strategy shows density closer to the conventional AISI 316L material, which is 8.0 kg/cm³ [22]. That might also be related with the higher amount of energy spent on that strategy.

Although density is expected to be lower than the conventional material due to inevitable pores and voids inherent to the AM DED processes with no post processing for minimizing the voidage, all strategies tested presented considerable influence on material density.

Figure 7 shows a comparison amongst the typical microstructure aspect of those workpieces produced. Cuts were made to observe the cross sections of beads. They show the typical microstructure of welded materials.

It becomes evident that no actual voids can be noticed since the stepover was selected aiming at a dense material. Laser power was also correctly selected in order to blend layers melting them as much as possible. Figure 8 shows in more detail the junction between two adjacent beads with the lower layer.

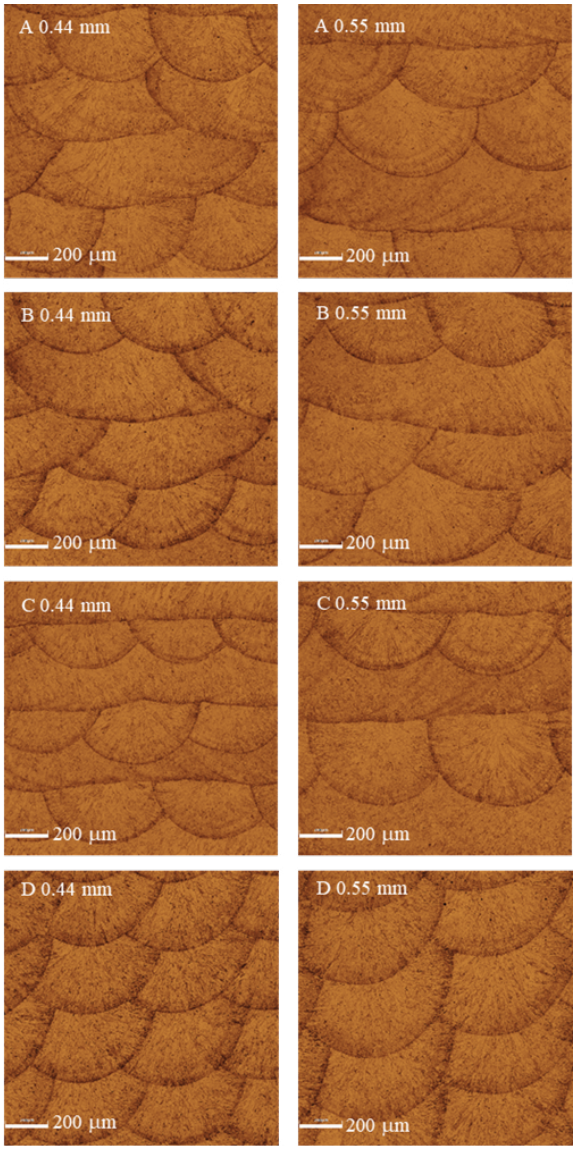

Fig. 7. Typical microstructure aspect of the produced workpieces.

It can be seen that the fusion with the lower layer was as good as between adjacent beads leaving no considerable voids and some few pores that could be spotted when scanning the polished surface. From microstructure examinations, it was also possible to notice grain orientations according to cooling direction and laser movement. Figure 9 shows some of those aspects.

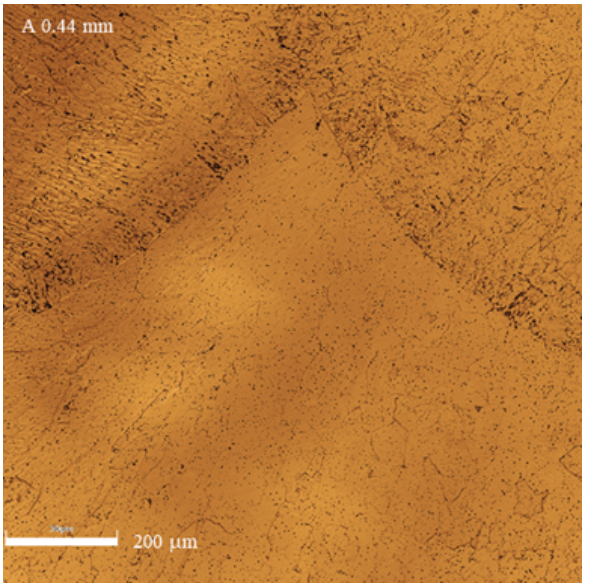

Fig. 8 – Details of a junction of two adjacent beads with the lower layer.

Table 2. Density of the deposited SS 316L considering different raster strategies and deposition stepover.

Raster strategy	Stepover (*mm*)	Density (g/cm^3)
Linear	0.44	7.781
	0.55	7.720
Zigzag	0.44	7.460
	0.55	7.714
Chessboard	0.44	7.721
	0.55	7.820
Contour	0.44	7.873
	0.55	7.919

In Figure 9(a) it is possible to see the grains all inclined which suggests that laser was running from right to left, since grains started to solidify from the bottom to the upper part of each bead. Figure 9(b) shows a different part of the same strategy (contour) where cross and longitudinal sections of the same layers can be seen. On the cross section, grains tend to grow from the bottom to the center, since the melt pool might have a round bottom and solidifies from the periphery to the center. That happens since heat is first lost to the layer below and to the bead on the side.

Microhardness data for the different deposition strategies and stepover is presented in Figure 10 with bars for plus-minus 3 standard deviation. In Figure 10, one can see that linear, zigzag and chessboard deposition strategies have produced material with close microhardness properties, in the range between 218 and 228 HV. The contour strategy has produced workpiece with the lowest average value for microhardness (209 HV), which is also the closest to the annealed SS 316 [22]. One can see that the deposition strategy has strong influence on the mechanical properties. This can be due mainly to the difference in heat transfer rate and the overall thermal activity during deposition. As expected, contour strategy seems to have had the most uniform heat transfer of all.

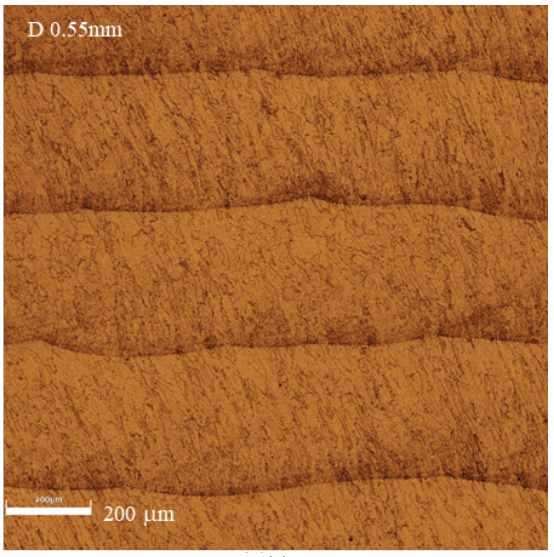

(a)

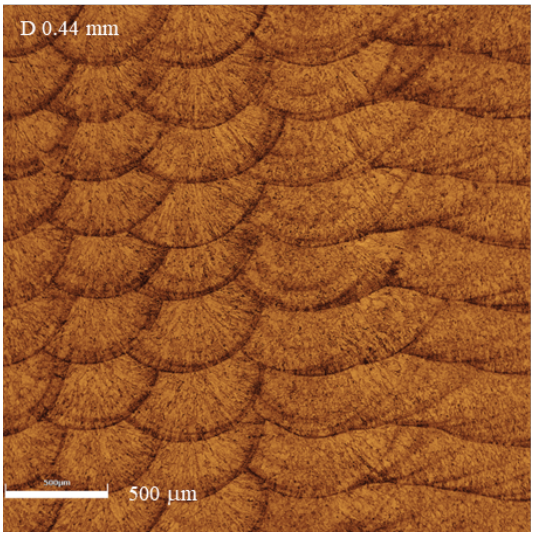

(b)

Fig. 9 – Particular aspects of contour strategy.

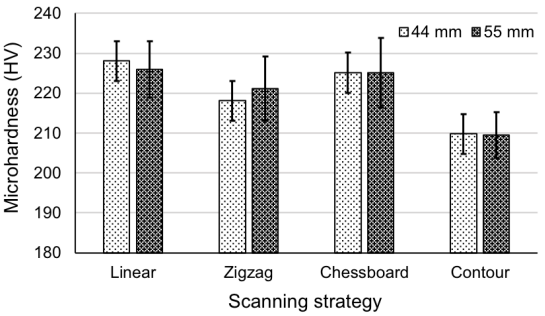

Fig. 10 – Microhardness of the produced workpieces.

5. Conclusions

From the particular set of experiments performed for this evaluation of the influence of toolpath strategy and stepover on deposited AISI 316L cubes, one can conclude that:

- all tested strategies presented differences on the upper cube edges geometry when comparing the stepover influence: flatter edges at the top were achieved by the 0.44 mm stepover strategies;
- contour strategy (helical-like) presented less distortions for the built cubic form regardless the toolpath stepover in comparison to the other strategies studied;
- deformation observed on the final workpiece geometry, as well as the presence of satellite powder can be associated to the thermal non-uniform distribution during deposition, which is strictly related to the raster strategy;
- regarding the roughness levels, it has been shown that linear and zigzag have no significant difference, contour presented the lowest Sa values, therefore the best surface finishing;
- the workpieces produced by zigzag, chessboard and contour raster strategies with the greater stepover have shown to be denser;
- contour strategy shows closer density to the SS 316L conventional material by achieving 7.919 g/cm³. It can be related to the amount of heat and its distribution during deposition;
- mechanical properties such as microhardness has shown to be influenced by the raster strategies. Out of the four, contour strategy, has produced workpieces with the closest hardness to the annealed SS 316. The evaluated stepovers have shown to not influence significantly the workpiece microhardness.

Acknowledgements

The authors are tankful to the São Paulo Research Foundation (FAPESP) for funding this work, and the research grant process n. 2019/00343-1. Also, thanks to BeAM Inc., in Cincinnati, Ohio, for the support on deposition.

References

[1] ASTM F2792-12a. Standard Terminology for Additive Manufacturing Technologies. West Conshohocken: ASTM International; 2013.

[2] Pinkerton A, Wang W, Li L. Component repair using laser direct metal deposition. Proc. IMechE Part B: J. Engineering Manufacture 2008;222:827-836.

[3] Thompson SM, Bian L, Shamsaei N, Yadollahi A. An overview of Direct Laser Deposition for additive manufacturing; Part I: Transport phenomena, modeling and diagnostics. Additive Manufacturing 2015;8:36-62.

[4] Toyserkani E, Stephen Corbin S, Khajepour A. Laser Cladding. 1st ed. Florida: CRC Press LLC; 2005.

[5] Bourell D, Kruth JP, Leu M, Levy G, Rosen D, Feese AM, Clare A. Materials for additive manufacturing. CIRP Annals 2017;66:659-681.

[6] Herzog D, Seyda V, Wycisk E, Emmelmann C. Additive manufacturing of metals. Acta Materialia 2016;117:371-392.

[7] Parimi LL, Ravi GA, Clark D, Attallah MM. Microstructural and texture development in direct laser fabricated IN718. Materials Characterization 2014;89:102-111.

[8] Michel F, Lockett H, Ding J, Martina F, Marinelli G, Williams S. A modular path planning solution for Wire + Arc Additive Manufacturing. Robotics and Computer-Integrated Manufacturing 2019;60:1-11.

[9] Li Y, Han Q, Zhang G, Horváth I. A layers-overlapping strategy for robotic wire and arc additive manufacturing of multi-layer multi-bead components with homogeneous layers. The International Journal of Advanced Manufacturing Technology 2018;96:3331-3344.

[10] Gong Y, Yang Y, Qu S, Li P, Liang C, Zhang H. Laser energy density dependence of performance in additive/subtractive hybrid manufacturing of 316L stainless steel. The International Journal of Advanced Manufacturing Technology 2019;105:1585-1596.

[11] Jhabvala J, Boillat E, Antignac T, Glardon R. On the effect of scanning strategies in the selective laser melting process. Virtual and Physical Prototyping 2010;5:99-109.

[12] Yu J, Lin X, Ma L, Wang J, Fu X, Chen J, Huang W. Influence of laser deposition patterns on part distortion, interior quality and mechanical properties by laser solid forming (LSF). Materials Science and Engineering 2011;528:1094-1104.

[13] Dai K, Shaw D. Distortion minimization of laser-processed components through control of laser scanning patterns. Rapid Prototyping Journal 2002;8:270-276.

[14] Ravi GA, Hao XJ, Wain N, Wu N, Attallah MM. Direct laser fabrication of three dimensional components using SC420 stainless steel. Material & Design 2013;47:731-736.

[15] Djuric A, Urbanic RJ. Using collaborative robots to assist with travel path development for material deposition based additive manufacturing processes. Computer-Aided Design and Applications 2018;15:542-555.

[16] Gilberti H, Sbaglia L, Urgo M. A path planning algorithm for industrial processes under velocityconstraints with an application to additive manufacturing. Journal of Manufacturing Systems 2017;43:160-167.

[17] Ding D, Pan Z, Cuiuri D, Li H, Larkin N. Adaptive path planning for wire-feed additive manufacturing using medial axis transformation. Journal of Cleaner Production 2016;133:942-952.

[18] Wang X, Wang A, Li Y. A sequential path-planning methodology for wire and arc additive manufacturing based on a water-pouring rule. The International Journal of Advanced Manufacturing Technology 2019;103:3813-3830.

[19] Zhao G, Ma G, Feng J, Xiao W. Nonplanar slicing and path generation methods for robotic additive manufacturing. The International Journal of Advanced Manufacturing Technology 2018;96:3149-3159.

[20] Zhang C, Chen F, Huang Z, Jia M, Chen G, Ye Y, Lin Y, Liu W, Chen B, Shen Q, Zhang, L, Lavernia EJ. Additive manufacturing of functionally graded materials. Materials Science and Engineering 2019;764:1-29.

[21] Spierings AB, Schneider M, Eggenberger R. Comparison of density measurement techniques for additive manufactured metallic parts. Rapid Prototyping Journal 2011;17:380-386.

[22] ASM International Handbook Committee. Metals Handbook. 10th ed. vol. 1. Novelty: ASM International; 1990.